https://doi.org/10.17221/380/2026-PSE

Long-term biogas slurry application drives molecular evolution of soil organic matter: from active input to stable sequestration

Lijun Liu[1], Xiuling Yu[2], Xiongzhen Lou[1], Yinxiu Liu[3], Peikun Jiang[1]**

[1]*College of Environment and Resources and College of Carbon Neutrality, Academic Affairs Office, Zhejiang A&F University, Hangzhou, P.R. China*
[2]*College of Environmental and Resource Sciences, Zhejiang University, Hangzhou, P.R. China*
[3]*Zhejiang Provincial Cultivated Land Quality and Fertiliser Administration Station, Hangzhou, P.R. China*
**Corresponding authors: 13958030270@163.com; jiangpeikun@zafu.edu.cn*

Citation: Liu L.J., Yu X.L., Lou X.Z., Liu Y.X., Jiang P.K. (2026): Long-term biogas slurry application drives molecular evolution of soil organic matter: from active input to stable sequestration. Plant Soil Environ., 72.

Abstract: The application of biogas slurry is known to enhance soil carbon storage, but the molecular-level processes driving the shift of soil organic matter (SOM) from labile inputs to stable forms remain unclear. To address this, we used a space-for-time substitution approach across agricultural soils receiving 0, 3, 5, and 10 years of continuous biogas slurry application. SOM molecular composition was analysed using pyrolysis gas chromatography/mass spectrometry (Py-GC/MS), combined with molecular indices such as average chain length of alkanes (ACL-ALK) and carbon preference index (CPI). Results showed that biogas slurry significantly increased soil organic carbon (SOC), mineral-associated organic carbon (MAOC), and particulate organic carbon (POC), with MAOC showing the greatest accumulation (176.32% increase over 10 years). Molecularly, slurry application altered aliphatic compounds – esters increased while phenols and olefins decreased. The molecular Shannon index rose initially, then declined, suggesting that prolonged disturbance drives SOM toward a new steady state. ACL-ALK and FA-L/S correlated positively with MAOC, while CPI correlated negatively with microbial biomass carbon (MBC), indicating that long-chain fatty compound enrichment is microbially mediated. Redundancy analysis identified MBC as the dominant factor controlling SOM molecular reconstruction, explaining 55.8% variation. Based on these findings, we propose a three-stage "active input-assimilation-stabilisation" framework to describe how biogas slurry facilitates SOC transition from active to stable pools. Overall, this study offers mechanistic insights into the carbon sequestration potential of reusing agricultural organic waste.

Keywords: organic waste recycling; agricultural organic amendment; pyrolysis-GC/MS; carbon stabilisation; molecular indicators

Soil organic matter (SOM) constitutes the largest carbon pool in terrestrial ecosystems, and its dynamics are critical for soil fertility (Liu et al. 2024), ecosystem functioning (Mou et al. 2025), and climate regulation (Khan et al. 2025). The application of exogenous organic amendments is widely adopted in agricultural production to improve soil quality and promote stable carbon sequestration (Bian et al. 2024). Among various organic amendments, biogas slurry has shown considerable potential for enhancing soil organic carbon (SOC) sequestration. For example, the application of anaerobically digested biogas slurry to cropland significantly increased SOC sequestration while reducing methane emissions by 7% compared with the control treatment (Moller et al. 2022); in a 9-year field experiment, continuous biogas slurry input promoted a more pronounced increase in particulate organic carbon (POC) and

© The authors. This work is licensed under a Creative Commons Attribution 4.0 International Licence (CC BY 4.0).

https://doi.org/10.17221/380/2026-PSE

mineral-associated organic carbon (MAOC) than afforestation (Ren et al. 2023); and similarly, within the 0–15 cm soil layer, biogas slurry application increased microbial biomass carbon (MBC), POC, and readily oxidisable organic carbon (ROC) by approximately 114, 245, and 75%, respectively, compared with nitrogen fertiliser application (Li et al. 2023). Although numerous studies have confirmed the positive effects of biogas slurry on SOC stocks and general soil properties, the molecular-scale transformation of organic matter derived from biogas slurry – that is, the potential mechanism by which active input materials are transformed into stable SOM – remains poorly understood. The knowledge gap limits our ability to evaluate the long-term stability and sequestration efficiency of SOC following exogenous inputs of organic carbon in agricultural soils.

Traditional physical fractionation methods for SOM, such as separating POC from MAOC, provide useful information for evaluating the stability of the soil carbon pool (Lavallee et al. 2020). However, these approaches cannot reveal the specific chemical pathways and molecular-scale compositional changes involved in carbon stabilisation. In recent years, molecular-marker-based analytical techniques have developed rapidly, providing opportunities to characterise SOM composition in greater depth (Du et al. 2025, Li et al. 2025), among which Py-GC/MS has become widely used for characterising complex molecular features of SOM (Lyu et al. 2024, Bonnefoy-Claudet et al. 2025). Based on Py-GC/MS data, a series of molecular indicators have been used to trace the sources, degradation status, and stabilisation pathways of organic matter. For instance, the ratio of unsaturated fatty acids $C_{16:1+2}$ to saturated fatty acid $C_{16:0}$ can indicate the presence of fresh plant tissues in soil (Harwood 1984); the ratio of fatty acids $C_{18:1-3}$ to $C_{18:0}$ can reflect the ongoing degradation process during the transformation of plant biomass into SOM (Wiesenberg et al. 2010); and the ratios of lignin-derived phenolic acids to their corresponding aldehydes within the vanillyl and coumaryl units can be used to assess the degradation stage of soil lignin (Otto et al. 2006). Nevertheless, for biogas slurry, a complex exogenous material produced through anaerobic digestion, it remains unclear whether its long-term input drives SOM evolution along a degradation-stabilisation pathway, similar to that of natural plant residues or through a more distinct transformation pathway.

This study hypothesised that long-term biogas slurry application would drive the molecular evolution of SOM from labile, slurry-derived compounds toward a stable pool enriched in persistent, less decomposable, or plant-derived aliphatic structures. To test this hypothesis, a space-for-time substitution approach was adopted. Agricultural soils receiving continuous applications of biogas slurry for 0, 3, 5, and 10 years were selected to establish a chronosequence. Soil physicochemical analyses and Py-GC/MS-based molecular fingerprinting were combined to: (1) quantify changes in total SOC and its fractions, including MAOC and POC; (2) characterise shifts in SOM molecular composition and molecular diversity; and (3) explore molecular stabilisation pathways by tracing the dynamics of key molecular indicators, including the average chain length of alkanes and fatty acids (ACL), CPI, and the ratio of long-chain to short-chain fatty acids (FA-L/S). By linking temporal changes in these molecular indicators to variations in soil carbon fractions, this study provides mechanistic evidence at the molecular level for the transition of SOM from active input to stable sequestration in biogas-slurry-amended soils.

MATERIAL AND METHODS

Site description, experimental design and soil sampling. The experimental site was located at Yuxi Lianye pig farming base in Changcheng Village, Heping Town, Changxing County, Huzhou City, Zhejiang Province, China (119°55'27.39'E, 30°51'5.14'N). The region is characterised by a subtropical monsoon climate, with abundant sunlight, mild temperatures, sufficient precipitation, distinct seasonal variation, concurrent rainfall and heat, and a favourable coordination between thermal and light conditions. The mean annual temperature is approximately 15.6 °C, with an interannual variation of ± 0.5~0.7 °C, and the mean annual precipitation is approximately 1 309 mm. The dominant soil types at the site are red soil and paddy soil.

To investigate the effects of long-term biogas slurry application on soil properties, this study adopted a space-for-time substitution approach. Adjacent cropland plots that had received continuous biogas slurry application for 0, 3, 5, and 10 years were selected to establish a chronosequence representing the cumulative effects of biogas slurry input. The initial soil samples collected and retained from each plot at the time of establishment were determined to be highly uniform in physicochemical properties (Table 1). The test biogas slurry was sourced from

https://doi.org/10.17221/380/2026-PSE

Table 1. Initial soil physicochemical properties of plots corresponding to each treatment before experimental setup

Indicator	0 year	3 years	5 years	10 years
pH	7.25 ± 0.08[a]	7.24 ± 0.03[a]	7.23 ± 0.07[a]	7.26 ± 0.05[a]
AHN (mg/kg)	128.56 ± 5.21[a]	130.12 ± 4.89[a]	131.45 ± 6.03[a]	129.78 ± 5.54[a]
AP (mg/kg)	21.82 ± 0.65[a]	22.05 ± 0.58[a]	22.31 ± 0.72[a]	21.94 ± 0.61[a]
AK (mg/kg)	188.45 ± 5.32[a]	190.12 ± 6.11[a]	191.36 ± 5.78[a]	189.67 ± 4.95[a]
SOC (g/kg)	12.98 ± 0.15[a]	13.05 ± 0.12[a]	13.11 ± 0.16[a]	13.02 ± 0.14[a]

Values are means ± standard deviations, n = 3. Different lowercase letters indicate significant differences among different years ($P < 0.05$). AHN – alkaline hydrolyzable nitrogen; AP – available phosphorus; AK – available potassium; SOC – soil organic matter

an anaerobic digestion system fed with pig manure and pen flushing wastewater, which was collected from a local pig farm. The annual application rate of biogas slurry was approximately 150 m^3/ha, applied fresh twice per year (once one week before rice transplanting and once one week before wheat sowing; applied by furrow application and immediately ploughed in, incorporated into the 0–20 cm soil layer), with the physicochemical properties of the biogas slurry kept as consistent as possible across years. The tested biogas slurry was weakly alkaline with a pH of 7.42. Its nutrient composition was as follows: total nitrogen (N) 0.10% (equivalent to 1.00 g/kg), hydrolysable nitrogen 855 mg/L (approximately 0.86 g/kg on a wet basis), total phosphorus (as P_2O_5) 0.05% (equivalent to 0.50 g/kg) and total potassium (as K_2O) 0.07% (equivalent to 0.70 g/kg). The organic matter content was 0.24%, and the chemical oxygen demand (COD) was 6.29 g/L. The moisture content of the biogas slurry was approximately 97%; its density was assumed to be approximately that of water, and organic carbon was calculated as 58% of the organic matter mass (Van Bemmelen factor). Based on these values, the annual carbon input from biogas slurry was estimated to be approximately 208.8 kg/ha, and the N input was 150 kg/ha.

Four treatments were established: no biogas slurry application (hereafter referred to as the 0-year control); continuous biogas slurry application for 3 years; continuous biogas slurry application for 5 years; and continuous biogas slurry application for 10 years. Each treatment included three replicate plots. A completely randomised block design was adopted. A single contiguous, homogeneous field was physically divided by ridges into 12 independent plots, with plastic film inserted down to the plough pan to prevent nutrient flow between plots (Figure 1). Each of the 4 treatments had 3 replicates, for a total of



Figure 1. Schematic diagram of the experimental plot layout. 0-year, 3-year, 5-year and 10-year represent soils receiving biogas slurry application for 0, 3, 5, and 10 years, respectively. Each treatment included three replicated plots

https://doi.org/10.17221/380/2026-PSE

12 independent plots (3 × 4). All plots had identical mineral-fertiliser field management for more than 10 years before this chronosequence experiment started in 2015. At the onset of the experiment in 2015, plots were randomly allocated to four treatments. From 2015 onward: the 10-year treatment received annual biogas-slurry input continuously from 2015 to 2025; the 5-year treatment received mineral fertiliser during 2015–2020 and then biogas-slurry during 2021–2025; the 3-year treatment received mineral fertiliser during 2015–2022 and biogas-slurry during 2023–2025; the 0-year control received mineral fertiliser across the whole 2015–2025 period.

During the 10 years, all plots were under a rice-winter wheat double-cropping rotation. All treatments followed local conventional fertilisation rates (annually, 240 kg N/ha, 33 kg P/ha, 125 kg K/ha) to ensure identical total macronutrient inputs across treatments. For biogas slurry treatments, nutrients carried by biogas slurry were counted toward the total supply, and supplementary mineral fertilisers were added to match the conventional rates. Other field practices, including irrigation, tillage and pest management, were completely uniform across all plots.

Combined with crop yield and root-to-shoot ratio (rice root-to-shoot ratio 0.12, wheat root-to-shoot ratio 0.15, straw return rate 50%), the annual carbon input from plant residues was estimated to be approximately 5.0–5.2 t/ha, and the total nitrogen input was approximately 73–76 kg/ha, with no significant differences among treatments (Table 2, $P > 0.05$).

Soil samples were collected after crop harvest. In each plot, no fewer than five sampling points were arranged in an S-shaped pattern, and soil samples were collected from the 0–30 cm soil layer. Samples from the same plot were thoroughly mixed to form one composite replicate sample. After visible plant residues and stones were removed, each sample was divided into two subsamples: one fresh subsample was stored at 4 °C and used within one week for the determination of MBC; the other was air-dried in a cool, well-ventilated place, then ground and passed through a 0.15 mm sieve for the determination of routine soil chemical properties.

Determination of physical and chemical properties of soil. Soil physicochemical properties were analysed according to the methods described by Lu (2000). Soil pH was measured by a composite electrode after extraction with distilled water at a soil-to-water mass ratio of 1:2.5. Soil alkaline hydrolysable nitrogen (AHN) was determined using the alkaline hydrolysis diffusion method. Soil available phosphorus (AP) was extracted with hydrochloric acid-ammonium fluoride solution using the Bray method and then determined by the molybdenum-antimony colourimetric method. Soil available potassium (AK) was measured using flame photometry. SOC content was determined using the potassium dichromate external heating method. Dissolved organic carbon (DOC) was measured using a total organic carbon analyser (Shimadzu TOC-Vcph, Tokyo, Japan). MBC was determined using the same analyser after chloroform fumigation and potassium sulfate extraction. POC was determined with reference to the $(NaPO_3)_6$ dispersion and shaking method (Wu et al. 2021). Mineral-associated organic carbon was determined and calculated according to the method of Zhao et al. (2025). ROC was analysed using the modified Walkley-Black method (Xie et al. 2013).

Py-GC/MS analysis of soil organic matter. The molecular composition of soil organic matter was characterised using pyrolysis-gas chromatography/mass spectrometry (Py-GC/MS). Briefly, approximately 100 mg of air-dried soil sample was weighed into a quartz boat and moistened with 1 mL of 25% tetramethylammonium hydroxide (TMAH) in methanol. The sample was then purged and dried under a high-purity helium atmosphere for approximately 10 min. Subsequently, it was transferred into a Pyrex tubular reactor (50.0 cm × 3.5 cm) and pyrolysed at 400 °C for 30 min using a Barnstead Thermolyne 21100 pyrolysis furnace. The released pyrolysis products were continuously carried by helium at a flow rate of 100 mL/min into two trapping bottles, each containing 50 mL of chloroform. The chloroform extracts were

Table 2. Annual average crop yields of each group

Rice (t/ha)	8.52 ± 0.21[a]	8.61 ± 0.18[a]	8.75 ± 0.24[a]	8.63 ± 0.24[a]
Wheat (t/ha)	5.16 ± 0.15[a]	5.22 ± 0.13[a]	5.30 ± 0.17[a]	5.27 ± 0.16[a]

Values are means ± standard deviations, $n = 3$. Different lowercase letters indicate significant differences among different years ($P < 0.05$)

https://doi.org/10.17221/380/2026-PSE

combined in a round-bottom flask and concentrated by rotary evaporation. The residue was then redissolved in 1 mL of chloroform and transferred into a vial for instrumental analysis.

GC-MS analysis was performed on a Perkin-Elmer Autosystem XL gas chromatograph with an RTX-5MS WCOT capillary column (Restek, 30 m × 0.25 mm, film thickness 0.25 μm), which was connected to mina PE TurboMass Gold quadrupole mass spectrometer through a heated transfer line maintained at 300 °C. The mass spectrometer was operated in electron-impact ionisation mode at an ionisation energy of 70 eV. The ion source temperature was set at 230 °C, the quadrupole temperature at 150 °C, and the mass scan range at m/z 30~500.

The pyrolysis products were identified by matching their mass spectra against the National Institute of Standards and Technology (NIST) mass spectral library, published spectra, and authentic standards. Semi-quantification was performed using the percentage of each compound's peak area relative to the total peak area. The identified compounds were then classified into 12 categories according to similarities in precursor materials and chemical structures (Kov et al. 2018): olefins, alkanes, alcohols, esters, ethers, other aliphatic compounds, other compounds, amino acid N (AAN), other nitrogen-containing compounds, phenolic compounds (Ph), monocyclic aromatic compounds (Ar), and other aromatic compounds.

Calculations and statistics. All data were first tested for normality using the Shapiro-Wilk test and were then statistically analysed using SPSS 18.0 software (SPSS Inc., Chicago, USA). One-way ANOVA followed by Duncan's multiple range test was used to evaluate the significant effects of continuous biogas slurry application on basic soil physicochemical properties. Pearson correlation analysis and linear regression were further performed to explore changes in the molecular composition of soil organic carbon. A significance threshold of $P < 0.05$ was applied throughout.

Soil molecular proxies. Several soil organic carbon molecular proxies have been demonstrated to evaluate the sources, decomposition processes, and changes in molecule structures of SOM (Wiesenberg et al. 2010). In this study, the following molecular proxies were calculated (to minimise potential interference from extremely short- or long-chain contaminants, specific carbon-number ranges were defined for the calculations):

The average chain length of alkanes (ACL-ALK):

$$ACL\text{-}ALK = \frac{\Sigma(z_n \times n)}{\Sigma(z_n)}$$

where: z_n – relative abundance of alkanes with n carbon atoms, n ranging from 16 to 36. The average chain length of fatty acids (ACL-FA) was calculated in the same manner using the corresponding fatty acid compounds.

ACL can be used to evaluate the degradation process of soil organic matter. A lower ACL indicates a shorter average chain length, suggesting that these components have higher bioavailability and can be rapidly utilised by microorganisms. As degradation proceeds, short-chain fatty acids and alkanes are preferentially metabolised by microorganisms, leading to the enrichment of longer-chain aliphatic compounds that are structurally more stable and, consequently, an increase in ACL values (Otto et al. 2006).

Ratio of long chain *vs.* short chain fatty acids, FA-L/S:

$$FA\text{-}L/S = \frac{\sum C_{20-34}}{\sum C_{16-19}}$$

where: $C_{20\text{-}34}$ and $C_{16\text{-}19}$ – fatty acids with carbon-chain lengths of 20–34 and 16–19, respectively.

FA-L/S can be used to assess the degree of soil carbon stabilisation. Short-chain fatty acids, especially C_{16} and C_{18}, are dominant lipid components in both plant tissues and microorganisms (PostBeittenmiller 1996). Therefore, a lower FA-L/S value indicates the predominance of short-chain fatty acids in soil, suggesting strong microbial activity or fresh SOM input. As degradation proceeds, chemically stable compounds, such as long-chain plant waxes, tend to be preserved and stabilised, thereby contributing to a gradual increase in FA-L/S.

The carbon preference index (CPI) was calculated using a dual-offset averaging approach to minimise potential errors arising from chromatographic integration and injection variability. The CPI was determined as follows:

$$\boldsymbol{CPI} = 1/2\left(\frac{\sum C_{20+22+24+26+28+30}}{\sum C_{19+21+23+25+27+29}} + \frac{\sum C_{20+22+24+26+28+30}}{\sum C_{21+23+25+27+29+31}}\right)$$

where: the subscript of C_n denotes the corresponding carbon number of fatty acids.

The carbon preference index (CPI) is a useful indicator of the degree of organic matter degradation and the intensity of microbial activity. In fresh plant-derived organic matter, a distinct biosynthetic preference for

https://doi.org/10.17221/380/2026-PSE

Table 3. Basic physicochemical properties of soil after continuous application of biogas slurry

Indicator	0 year	3 years	5 years	10 years
pH	7.22 ± 0.10^{a}	7.19 ± 0.03^{a}	7.14 ± 0.02^{ab}	7.06 ± 0.01^{b}
AHN (mg/kg)	133.16 ± 6.39^{b}	143.98 ± 6.67^{b}	148.74 ± 14.78^{ab}	169.53 ± 17.10^{a}
AP (mg/kg)	22.57 ± 0.71^{c}	32.61 ± 0.60^{b}	43.07 ± 0.90^{a}	16.40 ± 1.49^{d}
AK (mg/kg)	192.00 ± 6.56^{d}	215.33 ± 9.50^{c}	241.67 ± 11.50^{b}	289.00 ± 12.53^{a}
SOC (g/kg)	13.32 ± 0.18^{d}	14.64 ± 0.12^{c}	16.22 ± 0.12^{b}	18.71 ± 1.01^{a}

Values are means ± standard deviations, n = 3. Different lowercase letters indicate significant differences among different years (P < 0.05). AHN – alkaline hydrolysable nitrogen; AP – available phosphorus; AK – available potassium; SOC – soil organic matter

even-carbon-numbered fatty acids is observed (Espelie et al. 1980, Wiesenberg et al. 2010), resulting in a higher proportion of even-chain homologues and thus a high CPI value. As organic matter undergoes prolonged microbial decomposition in soil, this biosynthetic signature is progressively attenuated, leading to a decline in CPI values toward unity (i.e., no chain-length preference). Consequently, lower CPI values reflect a more advanced stage of microbial degradation and stronger microbial metabolic activity.

RESULTS

Effects of continuous application of biogas slurry on soil physicochemical properties. Long-term application of biogas slurry had significant effects on soil fertility indicators and organic carbon fractions (Table 3). Soil pH decreased with increasing years of biogas slurry application, and the value after 10 years was significantly lower than that in the 0-year treatment (P < 0.05), although the soil remained weakly alkaline overall. In terms of soil nutrients, compared with the 0-year control, 10 years of biogas slurry application significantly increased the AHN content from 133.16 mg/kg to 169.53 mg/kg (P < 0.05), while AK increased by 50.52%. AP showed a nonlinear pattern; however, it initially reached a peak of 43.07 mg/kg during the 5-year treatment, then declined dramatically to 16.40 mg/kg after 10 years of application.

Long-term biogas slurry input significantly increased SOC content (P < 0.05), which rose continuously from 13.32 g/kg to 18.71 g/kg. Compared with the control, SOC increased cumulatively by 1.32, 2.90, and 5.39 g/kg after 3, 5, and 10 years of application, respectively, with average annual accumulation rates

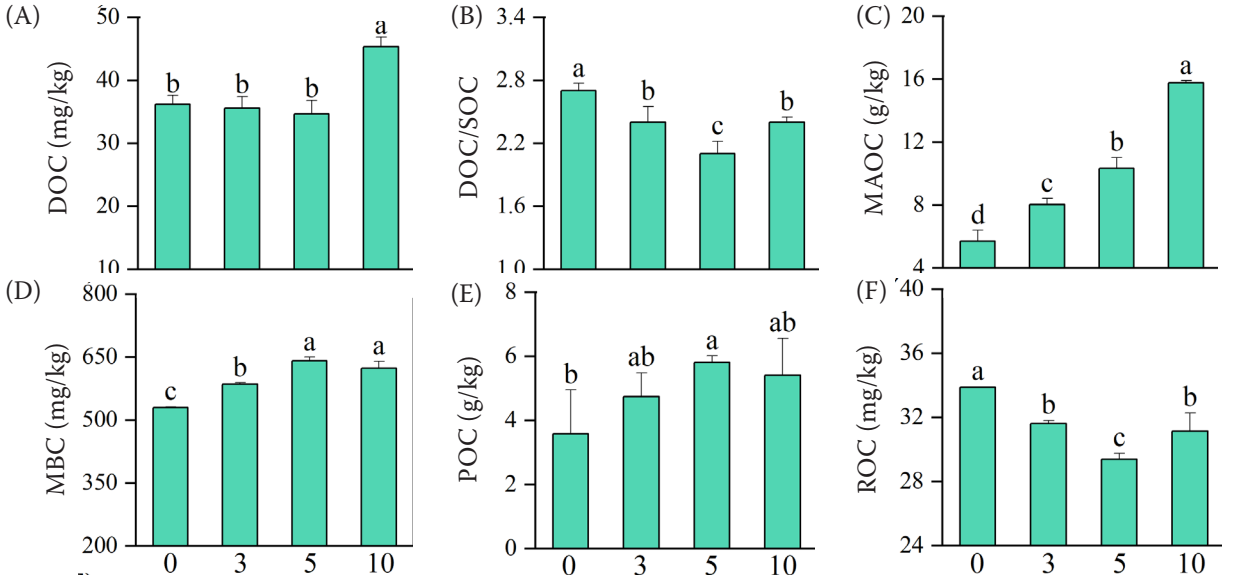

Figure 2. Changes in (A) the contents of soluble organic carbon; (B) the ratio of soluble organic carbon to soil organic carbon; (C) mineral-bound organic carbon, (D) microbial biomass carbon; (E) particulate organic carbon, and (F) readily oxidisable organic carbon in the soil under different durations of biogas-slurry application 0, 3, 5 and 10 represent soils with biogas-slurry application durations of 0, 3, 5, and 10 years, respectively. Different lowercase letters indicate significant differences among different years (P < 0.05), n = 3

https://doi.org/10.17221/380/2026-PSE

of 0.44, 0.58, and 0.54 g/kg. Among the fractions, MAOC showed the highest accumulation, increasing by 10.05 g/kg (176.32%) relative to the control at 10 years, and was the main fraction contributing to the SOC increase; POC increased cumulatively by 1.97 g/kg (51.12%) at 10 years.

Further analysis of soil organic carbon fractions revealed: that DOC remained relatively stable during the first 5 years but increased significantly ($P < 0.05$) after 10 years (Figure 2); POC reached its highest value in the 5-year treatment, at 5.81 g/kg, which was significantly higher than that in the 0-year control ($P < 0.05$); MAOC, in contrast, showed the strongest cumulative response ($P < 0.05$), steering its way from 5.70 g/kg to 15.75 g/kg, hence the major fraction driving the increase in total SOC. In addition, ROC, an indicator of the labile organic carbon pool, first decreased and then increased after biogas slurry application. It reached the lowest value of 29.40 mg/kg at 5 years and then increased slightly after 10 years, but remained significantly lower than in the control ($P < 0.05$). The DOC/SOC ratio also first decreased and then increased, reaching the lowest value of 2.1×10^{-3} in the 5-year treatment before increasing significantly to 2.4×10^{-3} in the 10-year treatment ($P < 0.05$).

Effects of continuous biogas slurry application on molecular structure of SOM. A total of 45, 81, 128, and 103 distinct molecular compounds were identified in soil organic matter from the 0-, 3-, 5-, and 10-year treatments, respectively. The pyrolysis products detected across all samples were classified into 12 categories: olefins, alkanes, alcohols, esters, ethers, other aliphatic compounds, other compounds, amino acid nitrogen, other nitrogen-containing compounds, phenolic compounds, monocyclic aromatic compounds, and other aromatic compounds. The relative abundance of each compound class is shown in Figure 3. The pyrolysis products were mainly composed of alkanes, olefins, alcohols, esters, other aliphatic compounds, other nitrogen-containing compounds, and other compounds, which together accounted for more than 85% of the total identified compounds in each soil sample. Compared with the 0-year control, the relative abundance of phenolic compounds decreased significantly by 66.86, 77.86, and 77.10% after 3, 5, and 10 years of continuous biogas slurry application, respectively ($P < 0.05$). Olefins decreased by 18.30, 34.58, and 39.17%, respectively, while alcohols decreased by 30.22, 22.79, and 49.91%. The relative abundance of other nitrogen-containing compounds in the 10-year treatment was significantly lower than that in the control ($P < 0.05$). In contrast, esters increased significantly with biogas slurry application ($P < 0.05$), reaching the highest relative abundance of 32.04% after the 5-year treatment.

The pyrolysis products were grouped into four broader categories according to their possible sources and chemical structures: aliphatic compounds, including olefins, alkanes, esters, ethers, alcohols, etc.; aromatic compounds, including phenolic compounds, monocyclic aromatic compounds, etc.; nitrogen-containing compounds, including amino acid nitrogen, etc.; and others, including halogenated hydrocarbons and other compounds. The relative abundance of aromatic compounds decreased gradually with increasing years of biogas slurry application. Compared with the 0-year control, aromatic compounds decreased by 49.06, 48.86, and 36.40% after 3, 5, and 10 years of application, respectively ($P < 0.05$) (Figure 4). The abundance of nitrogen-containing compounds showed an initial increase, followed by a decrease,

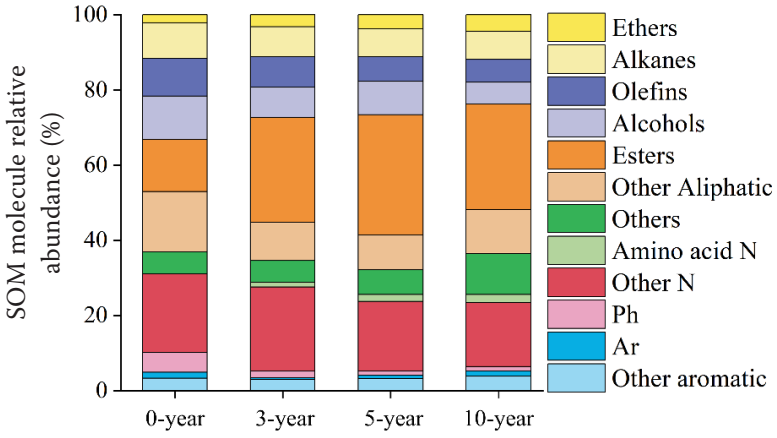

Figure 3. Changes in the relative abundance of soil organic carbon (SOM) molecular classes in soils under different durations of biogas-slurry application. 0-year, 3-year, 5-year and 10-year represent soils with biogas-slurry application durations of 0, 3, 5, and 10 years, respectively. Others refer to miscellaneous unclassified compounds; other compounds; amino acid N – amino acid nitrogen; other N – other nitrogen-containing compounds; Ph – phenolic compound; Ar – monocyclic aromatic

https://doi.org/10.17221/380/2026-PSE

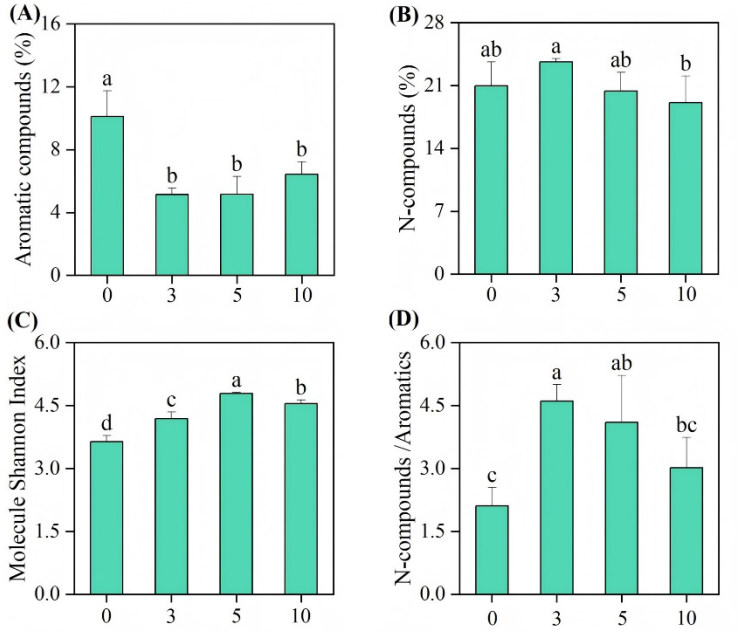

Figure 4. Changes in the (A) relative abundance of aromatic compounds; (B) nitrogen-containing compounds; (C) molecule Shannon index, and (D) the ratio of N-compounds to aromatic compounds in soils under continuous biogas-slurry application. 0, 3, 5, and 10 represent soils with biogas-slurry application durations of 0, 3, 5, and 10 years, respectively. Different lowercase letters indicate significant differences among different years ($P < 0.05$), $n = 3$

rising significantly from 20.95% in the 0-year control to 23.62% in the 3-year treatment ($P < 0.05$), then gradually declining to the lowest value of 19.10% in the 10-year treatment. Biogas slurry input significantly increased the molecular Shannon index ($P < 0.05$), which peaked at 4.78 in the 5-year treatment. The ratio of nitrogen-containing compounds to aromatic compounds increased rapidly in the 3-year treatment ($P < 0.05$), then gradually declined, showing no significant difference from the 0-year control by the 10-year treatment.

Soil molecular proxies were calculated from Py-GC/MS results to evaluate the transformation of SOM. As shown in Figure 5A, long-term biogas slurry input significantly increased ACL-ALK and ACL-FA in soil ($P < 0.05$). Specifically, ACL-ALK reached its highest value at 25.14 after 5 years of biogas slurry application, which was significantly higher than that in the 0-year control (18.53; $P < 0.05$), and then showed a slight decline. ACL-FA exhibited a cumulative response (Figure 5B), reaching its highest value in the 10-year treatment, corresponding to

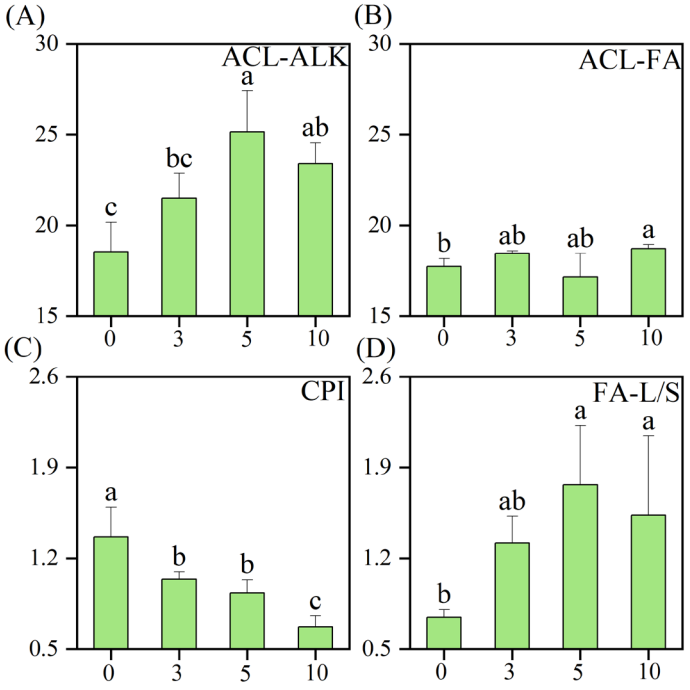

Figure 5. Changes in the soil molecular indicators: (A) average chain length of alkanes (ACL-ALK); (B) fatty acids (ACL-FA); (C) carbon preference index (CPI), and (D) ratio of long-chain to short-chain fatty acids (FA-L/S) under different durations of biogas-slurry application. 0, 3, 5, and 10 represent soils with biogas-slurry application durations of 0, 3, 5, and 10 years, respectively. Different lowercase letters indicate significant differences among different years ($P < 0.05$), $n = 3$

https://doi.org/10.17221/380/2026-PSE

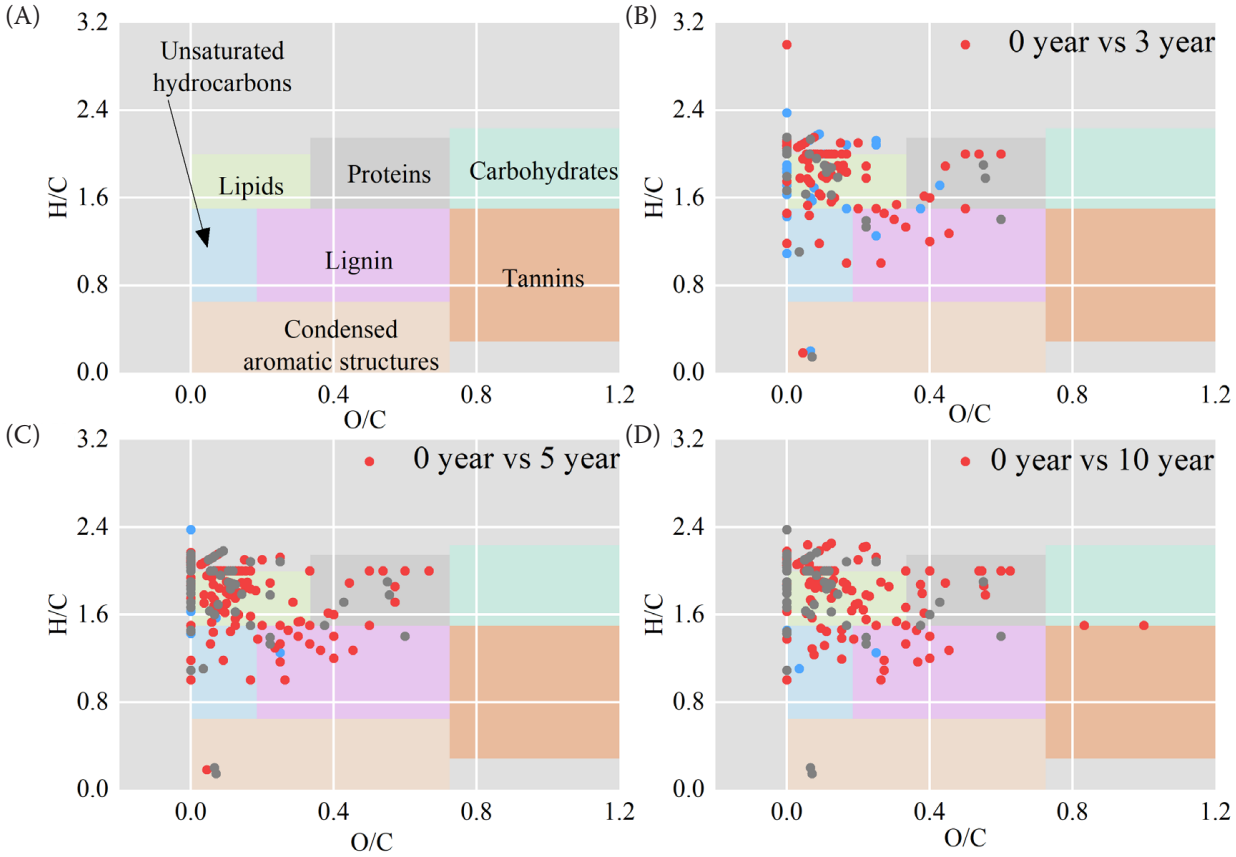

Figure 6. Van Krevelen diagrams of the molecular distribution of soil organic matter chemical structure for (B) 0-year comparison with 3-year application of biogas slurry, (C) with 5-year application of biogas slurry, and (D) with 10-year application of biogas slurry. Blue dots represent the same molecules, red dots represent newly added molecules, and gray dots represent molecules that have disappeared

105.47% of the control value. As shown in Figure 5C, CPI, which characterises the predominance of even-carbon fatty acids over odd-carbon fatty acids, decreased with biogas slurry application, hence the CPI in 10-year treatment significantly lower than that in 0-year control, decreasing by 50.82% ($P < 0.05$); and as in Figure 5D, FA-L/S which reflects the retention of chemically stable long-chain fatty acids such as plant waxes, gradually increased with biogas slurry input, and reached high levels in the 5- and 10-year treatments, increasing significantly by 136.35% and 105.11% against 0-year control, respectively ($P < 0.05$).

Based on the molecular fingerprints obtained with Py-GC/MS, Van Krevelen diagrams, expressed as the atomic H/C ratio *versus* the atomic O/C ratio, were constructed to characterise the evolution of SOM molecular composition under long-term biogas slurry application (Figure 6). Based on the H/C and O/C ratios, the detected SOM pyrolysis products were classified into seven major compound categories: lipids, unsaturated aliphatics, proteins/amino sugars, carbohydrates, lignins, tannins, and aromatics (Figure 6A). The results showed that biogas slurry input markedly altered the molecular composition and diversity of SOM. Compared to the 0-year control, 84 new molecules appeared in the soil SOM after 3 years of application, while 24 molecules disappeared. This stage of molecular turnover was mainly associated with lipid compounds, including 62 newly detected lipid molecular features and 17 lipid molecular features that were no longer detected. As the application duration extended to 5 years, the disturbance to molecular composition became more pronounced. Compared with the 0-year control, 149 molecular compounds were detected in the 5-year treatment, among which lipids (71.14%) and lignins (11.41%) were dominant contributors. Meanwhile, 46 molecular compounds were no longer detected, mainly including 31 lipid compounds and 5 unsaturated aliphatic compounds. In addition, the number of shared mol-

https://doi.org/10.17221/380/2026-PSE

ecules across compound classes decreased sharply at this stage, signalling substantial reconstruction of the SOM molecular pool. After 10 years of biogas slurry application, 133 new molecular compounds were detected, with more diverse precursor sources. These newly formed molecules were mainly lipids (61.65%), proteins/amino sugars (16.54%), lignins (12.03%), and unsaturated aliphatics (8.27%). A total

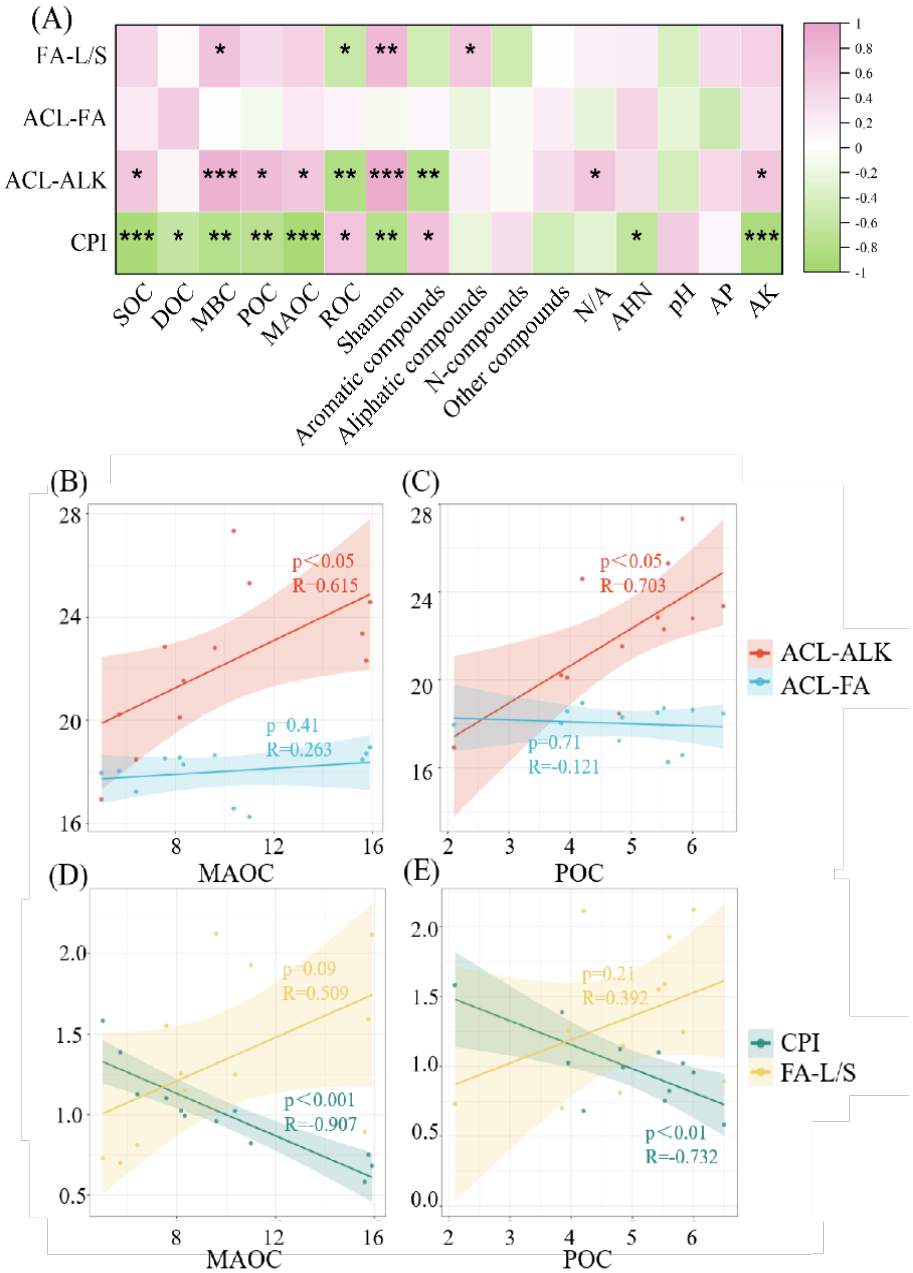

Figure 7. Correlation analysis among soil carbon fractions, molecular indicators, chemical composition, and physicochemical properties and linear regression analysis between mineral-associated organic carbon (MAOC), soil particulate organic carbon (POC) against molecular indicators SOC – soil organic carbon; DOC – dissolved organic carbon; MBC – microbial biomass carbon; POC – particulate organic carbon; MAOC – mineral-associated organic carbon; ROC – recalcitrant organic carbon; Shannon – Shannon diversity index; N-compounds – nitrogen-containing compounds; N/A – ratio of nitrogen-containing compounds to aromatic compounds; AHN – alkali-hydrolysable nitrogen; AP – available phosphorus; AK – available potassium; FA-L/S – ratio of long-chain to short-chain fatty acids; ACL-FA – average chain length of fatty acids; ACL-ALK – average chain length of alkanes. Red/blue color scale indicates positive/negative correlations. *$P < 0.05$; **$P < 0.01$; ***$P < 0.001$

https://doi.org/10.17221/380/2026-PSE

of 40 distinct molecular compounds were no longer detected, among which lipids remained dominant, accounting for 70%.

Relationships among SOM molecular proxies, carbon fractions, chemical composition, and physicochemical properties. The correlations among SOM molecular proxies and soil physicochemical properties are shown in Figure 7A. FA-L/S was significantly and positively correlated with MBC, aliphatic compounds, and SOM molecule diversity, as indicated by the Shannon index ($P < 0.05$), whereas it was significantly and negatively correlated with ROC ($P < 0.05$). ACL-ALK showed significant positive correlations with SOC, MBC, POC, MAOC, Shannon index, N/A, and AK ($P < 0.05$), but significant negative correlations with ROC and aromatic compounds ($P < 0.05$). CPI was significantly and positively correlated with ROC and aromatic compounds ($P < 0.05$). In contrast, it was significantly and negatively correlated with SOC, DOC, MBC, POC, MAOC, Shannon index, AHN, and AK ($P < 0.05$).

ACL-ALK was significantly and positively correlated with both MAOC and POC ($P < 0.05$), whereas ACL-FA showed no significant relationship with either fraction (Figure 7B, C). CPI was significantly and negatively correlated with both MAOC and POC ($P < 0.05$); FA-L/S showed a positive but non-significant trend with MAOC and POC (Figure 7D, E). RDA was performed to examine the relationships between soil indicators and the molecular composition of SOM (Figure 8). The first two RDA axes explained 63.60% and 16.37% of the total variation, together accounting for 79.97% of the explained variance. Samples from the 0-year control were clearly separated from those subjected to 3, 5, and 10 years of biogas slurry application along the RDA1 axis, indicating that biogas slurry application markedly altered the molecular composition of SOM.

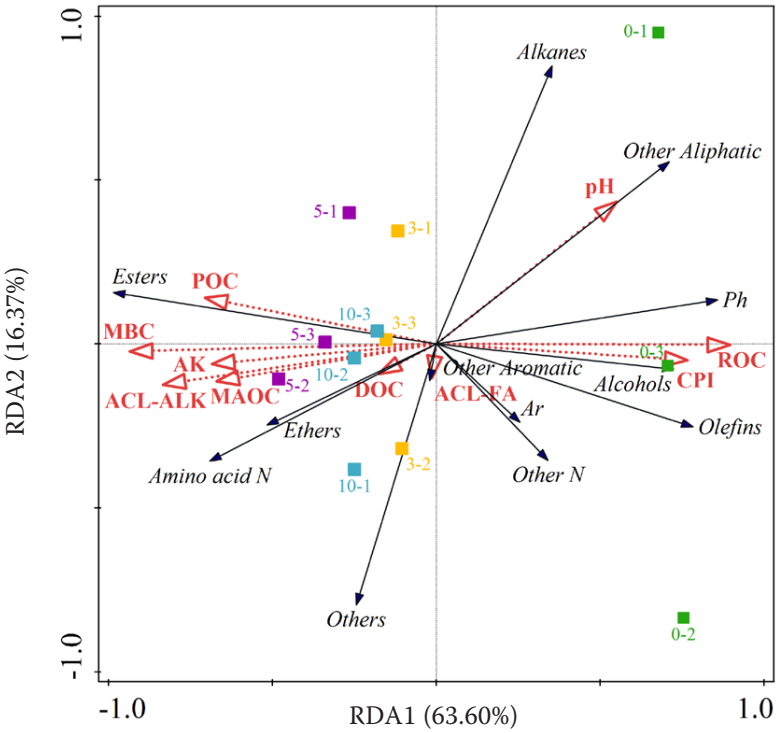

Figure 8. Redundancy analysis (RDA) of soil organic matter (SOM) molecular composition constrained by environmental factors and molecular indicators. Black arrows represent soil organic matter molecular compound classes (alkanes; other aliphatic; Ph – phenolic; alcohols; other aliphatic; olefins; other N, other nitrogen-containing compounds; Ar – monocyclic aromatic; others – other compounds; esters – amino acid N, amino acid nitrogen; ethers); Red arrows represent environmental factors and molecular proxies (pH; AK – available potassium; DOC – dissolved organic carbon; MBC – microbial biomass carbon; POC – particulate organic carbon; MAOC – mineral-associated organic carbon; ROC – recalcitrant organic carbon; CPI – carbon preference index; ACL-FA – average chain length of fatty acids; ACL-ALK – average chain length of alkanes). Coloured squares represent different durations of biogas slurry application: green = 0 years (control); yellow = 3 years; blue = 5 years; and purple = 10 years, with 3 replicates per treatment

https://doi.org/10.17221/380/2026-PSE

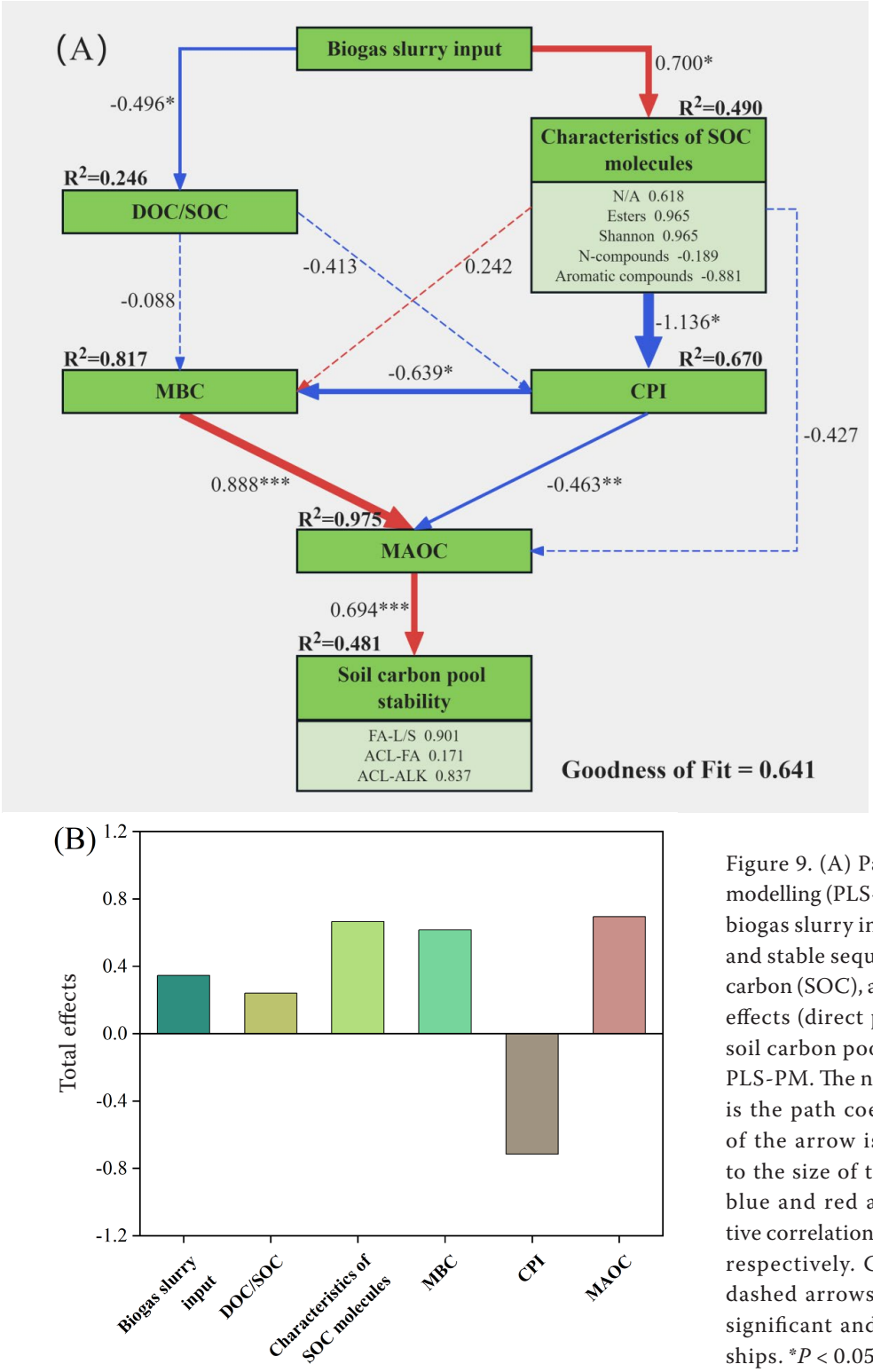

Figure 9. (A) Partial least squares path modelling (PLS-PM) displaying effects of biogas slurry input driving active input and stable sequestration of soil organic carbon (SOC), and (B) standardised total effects (direct plus indirect effects) on soil carbon pool stability derived from PLS-PM. The number next to the arrow is the path coefficient, and the width of the arrow is directly proportional to the size of the path coefficient. The blue and red arrows represent negative correlation and positive correlation respectively. Continuous arrows and dashed arrows respectively represent significant and insignificant relationships. *$P < 0.05$; **$P < 0.01$; ***$P < 0.001$

Marginal effects testing showed that MBC (explaining 55.8% of the variation, $P = 0.002$) and pH (explaining 8.7% of the variation, $P = 0.038$) were the main factors influencing the molecular composition of soil organic matter ($P < 0.05$). In the RDA biplot, MBC was positively correlated with esters, ethers, amino acid nitrogen, and other compounds; pH was positively associated with alkanes, other aliphatic compounds, phenolic compounds, alcohols, olefins, monocyclic aromatic compounds, and other nitrogen-containing compounds.

https://doi.org/10.17221/380/2026-PSE

DISCUSSION

Long-term biogas slurry input drives the augmentation of soil carbon stock. The results showed that long-term application of biogas slurry significantly increased soil carbon stocks (Table 1). Compared with the 0-year control, where biogas slurry was never applied, continuous biogas slurry input for 10 years increased SOC content by 40.47%. Specifically, the dramatic accumulation of MAOC, which increased by 176.32%, was the primary contributor, while POC also increased substantially by 51.12%. This trend accords with the findings of Liu et al. (2026) in regions with comparable climate and soil conditions, suggesting that exogenous carbon input can promote the simultaneous accumulation of POC and MAOC, thereby producing a carbon sequestration effect in temperate to tropical climates, clay paddy soils, and moderate cultivation intensity.

POC is mainly composed of light organic fragments derived from the physical fragmentation of plant residues, such as cellulose and hemicellulose. It has a relatively short turnover cycle and is generally considered a labile carbon pool (Lavallee et al. 2020). The observed increase in POC with the application of biogas slurry in this study (Figure 2E) may be attributed, on the one hand, to the direct input of incompletely decomposed organic particles contained in the biogas slurry per se; and on the other hand, to enhanced plant-derived carbon, including facilitated rhizodeposition and high-quality residue input, resulting from the positive effects of biogas slurry as an efficient organic fertiliser on plant growth (Xu et al. 2021, Mukhtiar et al. 2024). In addition, plant-derived carbon not only contributes directly to the formation of the POC pool but also indirectly participates in MAOC stabilisation by promoting the physical protection of soil aggregates and facilitating chemical bonding between minerals and organic compounds (Shang et al. 2026).

MAOC is a relatively stable carbon pool formed through the adsorption of low-molar-mass compounds, such as microbial metabolites and plant leachates, onto mineral surfaces. Its physical association and chemical bonding with minerals result in a very slow turnover rate, making MAOC a core participant in long-term soil carbon sequestration (Lavallee et al. 2020, Lugato et al. 2021). In this study, the MAOC content increased significantly year by year with the application of biogas slurry (Figure 2C). The accumulation mechanism can be analysed through two pathways: direct and indirect. Directly, DOC and other dissolved components contained in biogas slurry that are yet to be utilised by microorganisms may participate in MAOC formation through specific adsorption onto reactive sites on mineral surfaces *via* functional groups such as carboxyl and hydroxyl (Fan et al. 2024). Indirectly, microbial transformation plays a key role, while soil environmental factors may also function as important regulators. Biogas slurry input can stimulate microbial growth and metabolism (Cai et al. 2024). This is consistent with our experimental results (Figure 2D). Microbial-derived residues may subsequently be stabilised on mineral surfaces through chemical bonding, for example through associations with Fe/Al oxides, thereby contributing to MAOC accumulation (Yang et al. 2022, Liao et al. 2023). Meanwhile, in terms of soil environmental factors, a decrease in pH may lead to the leaching of base cations such as Ca and Mg, thereby increasing the chance of direct binding between microbial-derived compounds and minerals, for example through ligand exchange (Liao et al. 2023, Yu et al. 2024), which is also in keeping with the significant decrease in soil pH ($P < 0.05$) observed in this study (Table 1). Moreover, paddy soil type, clayey texture, and water management characteristics of the experimental site may have further strengthened MAOC stabilisation, for clayey texture favours the formation and accumulation of organo-mineral complexes (Zhou et al. 2024, Liu et al. 2025); flooded paddy soil creates anaerobic conditions that slow organic carbon decomposition (Moyano et al. 2013); while wetting-drying cycles may also promote the formation of amorphous minerals, such as poorly crystalline Fe/Al oxides, which readily adsorb organic carbon and facilitate MAOC formation (Xu et al. 2023).

Increase in labile carbon and the reconstruction of SOM composition driven by biogas slurry input. As an exogenous organic amendment, biogas slurry can supply substantial amounts of labile carbon to soil. This effect may be explained by four potential pathways. First, the abundant lipid compounds contained in biogas slurry may directly contribute to the expansion of the labile carbon pool (Tambone et al. 2013). After 3 years of biogas slurry application, 62 newly appeared lipid types were detected, accounting for 73.81% of all newly appeared molecules, as shown in the Van Krevelen diagram (Figure 6). This provides direct molecular evidence that biogas slurry, as an anaerobic fermentation product, contributes to the enrichment of the soil

https://doi.org/10.17221/380/2026-PSE

labile carbon pool. Second, biogas slurry contains relatively high levels of labile nitrogen compounds (Liu et al. 2024), which may enter soils along with slurry input and thereby increase the availability of labile carbon substrates. The results showed that nitrogen compounds (Figure 4C) increased during the early stage but then gradually decreased in the later stage, supporting the role of biogas slurry as an initial source of labile nitrogen compounds. In addition, the ratio of nitrogen compounds to aromatic compounds also showed an initial increase followed by a subsequent decrease (Figure 4D), reflecting substrate quality, with higher values indicating higher substrate quality (Lavallee et al. 2020), and further supporting the labile input from biogas slurry. Third, biogas slurry input significantly increased MBC by 15.2–20.9% (Figure 2D), thereby stimulating soil microbial activity and indirectly promoting the activation of the soil carbon pool. This activation effect was mainly reflected in the degradation of aromatic compounds. Specifically, the relative abundance of aromatic compounds decreased significantly ($P < 0.05$) after 3 years of biogas slurry input (Figure 4A), with phenolic compounds being the major class responsible for this decline ($P < 0.05$). Moreover, the relative abundance of phenolic compounds was negatively correlated with MBC but positively correlated with ROC and CPI (Figure 8). It may therefore be explained that ROC derived from biogas slurry may stimulate microorganisms to secrete lignin-degrading enzymes, such as peroxidases and laccases (Khan et al. 2019, Liang et al. 2024), thereby accelerating the decomposition of relatively simple lignin compounds (Wen et al. 2025). The low-molar-mass labile organic compounds produced therein are then partly assimilated by microorganisms to form MBC (Duan et al. 2025, Zhang et al. 2025), while the remaining compounds accumulate in soil. The decrease in CPI further indicates the weakening of even-over-odd carbon-number predominance and a gradual enhancement of microbial activity. Fourth, the slight decrease in soil pH from 7.22 to 7.06 ($P < 0.05$) shown in Table 3 may have promoted the release of labile carbon. A more acidic soil environment may facilitate the transfer of partially MAOCed carbon into POC, thereby increasing the labile carbon pool (Wang et al. 2025). It may also promote the growth of acidophilic microbial groups, thus altering the transformation rates and pathways of organic carbon (Li et al. 2025).

Driven by labile carbon input, the molecular composition of SOM was substantially reconstructed. More specifically, this reconstruction was mainly reflected in trade-offs among aliphatic compounds, with esters being the dominant compounds showing increased relative abundance ($P < 0.05$, Figure 2). In the RDA results, MBC was positively associated with esters (Figure 8), suggesting that ester accumulation may be linked to microbial synthesis of ester-containing derivatives, such as cell membrane components and extracellular secretions (Zhu et al. 2023). POC was also positively associated with esters (Figure 8), which may be because POC, as a labile carbon pool composed of plant residue fragments and microbial aggregates, has a relatively loose structure that provides physical protection for microbial products such as esters (Six et al. 2002), and therefore creates favourable conditions for ester accumulation. In addition, esters or their precursors carried by the biogas slurry itself are introduced directly into the soil upon application (Gao et al. 2026), thereby constituting a direct source of soil ester compounds.

As shown in Figure 3, olefins and alcohols were the major compounds showing decreasing relative abundance ($P < 0.05$). This decline may be attributed to their relatively high microbial availability, as the unsaturated bonds in olefins (Conlette 2011) and the hydroxyl groups in alcohols (Kamble et al. 2005, Araújo et al. 2011) make these compounds more susceptible to microbial utilisation. Moreover, Van Krevelen diagram analysis (Figure 6) showed that, compared with the 0-year control, the proportion of molecules commonly appearing in all three biogas slurry treatments was less than 25%. This further confirms, from the perspective of chemical space, that SOM underwent pronounced molecular reconstruction following the application of biogas slurry.

The "gain-convergence" pattern of molecular diversity further supports the evolution of SOM molecule structure. The Shannon index first increased and then decreased, rising from a relatively low level in the 0-year control to a peak of 4.78 in the 5-year treatment, before declining slightly to 4.21 in the 10-year treatment. The initial increase may be attributed to the introduction of numerous new molecules through exogenous carbon input (Figure 6), which altered the original composition of SOC and reflected a diversity-enhancing "gain effect" of exogenous carbon input, consistent with findings of Sun et al. (2025). The slight decline in later stages may indicate that, after intense disturbance, part of the labile components was consumed by microorganisms, and the system gradually converged toward the next equilibrium dominated by relatively stable

https://doi.org/10.17221/380/2026-PSE

compounds, such as long-chain lipids. Although molecular diversity decreased slightly at this stage, it remained higher than in the control, indicating that the SOM pool had reached a more complex steady state.

Stable storage of SOM driven by long-term biogas slurry application. The results (Figure 5) indicate that dynamic changes in molecular indicators, including ACL-ALK, ACL-FA, and FA-L/S, provide critical evidence for the transformation pathway from active input to the stable sequestration of SOM, driven by biogas slurry application.

Compared with the 0-year control, ACL-ALK increased significantly after 10 years of biogas slurry application (Figure 5A), directly indicating the selective preservation and enrichment of chemically stable long-chain organic carbon in soil. Specifically, ACL-ALK rose significantly from 18.53 in the 0-year control to 25.15 in the 5-year treatment ($P < 0.05$), then slightly declined to 23.42 in the 10-year treatment, but remained significantly higher than the control. This change is particularly outstanding against the background of biogas slurry input dominated by short-chain alkanes (C_8-C_{16}) (Gu et al. 2025). The possible pathways underlying this increase may include the input of long-chain plant residues such as C_{27}-C_{31} plant waxes (Wiesenberg et al. 2010), and/or contributions from microbial synthesis, as indicated by the significantly positive correlation between MBC and ACL-ALK (Figure 7A). Moreover, linear regression analysis (Figure 7B) shows that ACL-ALK is significantly positively correlated with both MAOC and POC, likely because MAOC can adsorb hydrophobic, recalcitrant long-chain alkanes (Schmidt et al. 2011), while particulate plant residues in POC carry long-chain alkanes, together providing favourable conditions for the increase in ACL-ALK.

The concurrent increases in ACL-FA and FA-L/S provide further proof of the enrichment trend of long-chain structures. The experimental results show that ACL-FA increased significantly from 17.74 in the 0-year control to 18.71 in the 10-year treatment ($P < 0.05$, Figure 5B), and FA-L/S rose from 0.75 to 1.53 ($P < 0.05$, Figure 5D), indicating a sustained increase in the relative abundance of C_{20}-C_{34} long-chain fatty acids. Such accumulation may be attributed to multiple sources: for example, undegraded or incompletely degraded plant cuticular waxes (C_{24}-C_{38}), suberin (C_{20}-C_{26}), and sphingolipids (C_{24}-C_{26}) potentially present in the biogas slurry (Batsale et al. 2023); input of recalcitrant C_{16}-C_{30} compounds from subterranean plant storage organs (Espelie et al. 1980); or stable membrane lipids synthesised by soil microorganisms during carbon transformation. Notably, the magnitude of increase in ACL-FA was generally lower than that of ACL-ALK, which is closely related to the fact that the fatty acids in biogas slurry are dominated by short-chain (C_2-C_4) and supplemented by medium-chain (C_5-C_6) compounds (Saritpongteeraka et al. 2014, Liu et al. 2022, Cui et al. 2024). Although the input of short-chain carbon compounds diluted the overall chain length, the net increase in long-chain components still dominated the rise in FA-L/S, reflecting a robust trend of the soil carbon pool transitioning toward a more stable state.

Microbial-driven mechanism model: from "active input" to "stable sequestration". The results of RDA and correlation analysis jointly revealed that MBC was the dominant environmental factor driving the evolution of SOM molecular composition (Figure 8), explaining 55.8% of the total variation in SOM, suggesting that MBC serves as the 'engine' reshaping SOM molecular structure. Specifically, biogas slurry input introduces readily utilisable short-chain organic carbon into the soil, stimulating microorganisms to metabolise these labile components preferentially. In contrast, the inherent or slurry-introduced long-chain, complex organic compounds are selectively retained owing to their high resistance to degradation, thereby driving the transformation pathway from active input to stable sequestration. The continuous decline in CPI to values below 1 further supports microbial-driven transformation processes (Figure 5C). CPI, defined as the ratio of even-carbon to odd-carbon fatty acids, approaches or falls below 1 when organic matter loses the natural biosynthetic signature of even-carbon-chain predominance; in contrast, naturally derived biogenic lipids typically exhibit CPI values greater than 2 (Wiesenberg et al. 2012). In this study, CPI decreased significantly from 1.37 in the 0-year control to 0.67 in the 10-year treatment ($P < 0.05$), indicating that the original predominance of plant-derived even-carbon-chain compounds was progressively weakened and that microbial transformation increasingly dominated the soil carbon pool. Quantitatively, CPI values dropped below 1, further supporting substantial de novo synthesis of odd-chain fatty acids, for example, in microbial phospholipid biosynthesis.

Based on the molecular dynamics described above, a three-stage conceptual model of SOM transformation under long-term biogas slurry input is proposed:

https://doi.org/10.17221/380/2026-PSE

(1) an active-input stage, characterised by the substantial input of ester compounds accompanied by supplementary inputs of nitrogen-containing compounds; (2) an assimilation stage, during which microorganisms rapidly utilise readily degradable labile organic carbon, thereby increasing MBC, with short-chain fatty acids, nitrogen-containing compounds, olefins, alcohols, and readily degradable phenolic compounds serving as the primary substrates; and (3) a carbon-pool stabilisation stage, in which the microbial community gradually approaches a new steady state, while MBC and molecular diversity reach a next equilibrium. During this stage, long-chain alkanes, long-chain fatty acids, and recalcitrant ester compounds progressively accumulate through mineral adsorption and stabilisation (MAOC increased by 176.32%) as well as particulate physical protection (POC increased by 51.12%).

In this study, PLS-PM was performed to quantify this mechanism (Figure 9A). The model illustrates the interactive relationships among biogas slurry input, the DOC/SOC ratio, SOM molecular characteristics, MBC, CPI, MAOC, and molecular indicators, with an overall goodness-of-fit (GoF) of 0.641. Specifically, biogas slurry input had a negative path coefficient with DOC/SOC but a positive path coefficient with SOM molecular characteristics. ($P < 0.05$). Changes in SOM molecular characteristics had a significant negative effect on CPI ($P < 0.05$), with 67.0% explained variance. CPI had a significant negative effect on MBC ($P < 0.05$), explaining 81.7% of the variance. MAOC was significantly negatively correlated with CPI ($P < 0.01$) and significantly positively correlated with MBC ($P < 0.01$). MBC and CPI jointly explain the changes in MAOC, with an explanatory variance of 97.5%. Soil carbon pool stability, assessed by FA-L/S, ACL-FA, and ACL-ALK, was overall significantly positively correlated with MAOC ($P < 0.001$), with an explained variance of 48.1%. From the standardised total effects perspective (Figure 9B), biogas slurry input positively increased carbon storage in the soil reservoir. Collectively, these results indicate that biogas slurry input alters SOM molecular structure and ultimately increases MAOC content and carbon pool stabilisation through MBC-mediated microbial transformation processes.

Overall, this study demonstrates that 10 years of continuous biogas-slurry input enhanced both the storage and stability of the soil carbon pool in subtropical paddy-wheat rotation red paddy soils. Obvious changes in SOM molecular composition were observed, with increased MAOC and MBC contents and decreasing relative abundances of aromatic and nitrogen-containing compounds. These findings clarify the sources of stable SOM carbon components and elucidate the transformation pathway through which exogenous carbon shifts from labile input to stable sequestration in this soil system. The results highlight that microbial activity is likely the primary driver of SOC stabilisation and sequestration for subtropical red paddy soils under paddy-wheat rotation.

Acknowledgment. We gratefully acknowledge the Zhejiang Provincial Farmland Quality and Fertiliser Management Station for providing the research facilities and infrastructure that supported this work.

REFERENCE

Araújo L.S., Kagohara E., Garcia T.P., Pellizari V.H., Andrade L.H. (2011): Screening of microorganisms producing cold-active oxidoreductases to be applied in enantioselective alcohol axidation: an antarctic survey. Marine Drugs, 9: 889–905.

Batsale M., Alonso M., Pascal S., Thoraval D., Haslam R.P., Beaudoin F., Domergue F., Joubès J. (2023): Tackling functional redundancy of Arabidopsis fatty acid elongase complexes. Frontiers in Plant Science, 14: 1107333.

Bian Q., Zhao L.X., Cheng K., Jiang Y.J., Li D.M., Xie Z.B., Sun B., Wang X.Y. (2024): Divergent accumulation of microbe- and plant-derived carbon in different soil organic matter fractions in paddy soils under long-term organic amendments. Agriculture Ecosystems and Environment, 366: 10.

Bonnefoy-Claudet C., Kaal J., Thevenot M., Panettieri M., Lévêque J., Mathieu O. (2025): Soil organic matter degradability as a function of forest species, a study based on Py-GC-MS analysis. Geoderma, 459: 12.

Cai J.B., Ran Q.F., Zhou J., Bi M., Liu Y., Yang S.S., Fan Y., Nie G., He W. (2024): Effects of arbuscular mycorrhizal fungi and biogas slurry application on plant growth, soil composition, and microbial communities of hybrid Pennisetum. Sustainability, 16: 15.

Conlette O.C. (2011): Aerobic degradation of paraffin and olefin synthetic-based drilling mud base fluids by Gulf of Guinea sediments under natural environmental conditions. Life Science Journal-Acta Zhengzhou University Overseas Edition, 8: 238–244.

Cui W.J., Meng J.Z., Wang S., Hu Z.H., Liu G.L., Zhan X.M. (2024): 17β-estradiol (E2) removal in anode-electrodialysis (anode-ED) during nutrient recovery from pig manure digestate. Journal of Hazardous Materials, 462: 9.

Don A., Schumacher J., Freibauer A. (2011): Impact of tropical land-use change on soil organic carbon stocks – a meta-analysis. Global Change Biology, 17: 1658–1670.

Du Z.L., Fu Q.L., Liu J.Y., Chai X.L., Wu B.R. (2025): Molecular humification mechanisms of dissolved organic matter during maize straw composting enhanced by humus soil biomaterial: paired-

https://doi.org/10.17221/380/2026-PSE

molecule mass difference reactomics analysis based on FT-ICR MS. Journal of Agricultural and Food Chemistry, 73: 21504–21515.

Duan F.Y., Tan F.X., Zhao X.M., Feng H., Wang J.K., Peng H., Zhang N.N., Huang Y.L. (2025): Microbial life strategies-mediated differences in carbon metabolism explain the variation in SOC sequestration between *Kandelia obovata* and *Sonneratia apetala*. Forest Ecosystems, 14: 11.

Espelie K.E., Sadek N.Z., Kolattukudy P.E. (1980): Composition of suberin-associated waxes from the subterranean storage organs of seven plants. Planta, 148: 468–476.

Fan J.L., Ge C.J., Li A.L., Ren G.L., Deng H., Wu D.M., Luo J.W., He Y.H., Zhao Y.Y., Li J.T., Feng D., Yu H.M. (2024): The structural transformation reversibility of biogas slurry-derived dissolved organic matter and its binding properties with norfloxacin under temperature fluctuation. Ecotoxicology and Environmental Safety, 271: 11.

Gao X.X., Yu X.Y., Jin C.Z., Jin L., Bu S., Li T.H., Ruan H.H., Shin K.S., Jin F.J. (2026): Long-term biogas slurry fertilization alters rhizosphere soil metabolite profiles and microbial communities in poplar plantations. Frontiers in Microbiology, 16: 16.

Gu Z.Q., Liu Y.H., Zhu L.D., Fan B.Y., Li Y., Liu C.X., Wang Y.P., Cui X., Yu Z.G., Ruan R., Zhang Q. (2025): Hormetic effect of dissolved organic matter from pig manure anaerobic digestion effluents on *Chlorella* sp.: physiological and transcriptomic responses. Water Research, 283: 14.

Harwood J.L. (1984): Lipids in Plants and Microbes. London, George Allen and Unwin.

Kamble A.L., Soni P., Banerjee U.C. (2005): Biocatalytic synthesis of S(-)-1-(1'-naphthyl) ethanol by a novel isolate of *Candida viswanathii*. Journal of Molecular Catalysis B-Enzymatic, 35: 1–6.

Khan M.T., Suproniene S., Zvirdauskiene R., Aleinikoviene J. (2025): Climate, soil, and microbes: interactions shaping organic matter decomposition in croplands. Agronomy-Basel, 15: 31.

Khan M.U., Ahring B.K. (2019): Lignin degradation under anaerobic digestion: influence of lignin modifications – a review. Biomass and Bioenergy, 128: 10.

Kov R., Camps-Arbestain M., Pereira R.C., Suárez-Abelenda M., Shen Q.H., Garbuz S., Vázquez F.M. (2018): A farm-scale investigation of the organic matter composition and soil chemistry of Andisols as influenced by land use and management. Biogeochemistry, 140: 65–79.

Lavallee J.M., Soong J.L., Cotrufo M.F. (2020): Conceptualizing soil organic matter into particulate and mineral-associated forms to address global change in the 21st century. Global Change Biology, 26: 261–273.

Li J.W., Chen L., Yue F.X., Zhang C.Z., Ma D.H., Zhou G.X., Wang J.L., Han C.D., Feng B., Zhang J.B. (2025): Microbiological mechanisms of lignin-and humus-derived small molecule addition promoting straw conversion into soil organic matter in a sodic soil. Pedosphere, 35: 603–616.

Li S., Wei W.L., Liu S.T. (2023): Long-term organic amendments combined with nitrogen fertilization regulates soil organic carbon sequestration in calcareous soil. Agronomy-Basel, 13: 17.

Li Z.X., Gao X.Y., Li D.D., Gao J., Li J.H., Cai Z.J., Sun N., Wu L.H., Xu M.G. (2025): Differential responses of bacteria, fungi, and C, N, P functions to soil acidification in farmland: a meta-analysis. Environmental Technology and Innovation, 40: 13.

Liang X.Y., Wang H., Wang C.J., Wang H.T., Yao Z.L., Qiu X.F., Ju H., Wang J.D. (2024): Unraveling the relationship between soil carbon-degrading enzyme activity and carbon fraction under biogas slurry topdressing. Journal of Environmental Management, 356: 15.

Liao J.J., Yang X., Dou Y.X., Wang B.R., Xue Z.J., Sun H., Yang Y., An S.S. (2023): Divergent contribution of particulate and mineral-associated organic matter to soil carbon in grassland. Journal of Environmental Management, 344: 12.

Liu M.L., Zheng S.L., Pendall E., Smith P., Liu J.J., Li J.Q., Fang C.M., Li B., Nie M. (2025): Unprotected carbon dominates decadal soil carbon increase. Nature Communications, 16: 8.

Liu Y., Ma R.A., Tang R.L., Kong Y.L., Wang J.N., Li G.X., Yuan J. (2022): Effects of phosphate-containing additives and zeolite on maturity and heavy metal passivation during pig manure composting. Science of the Total Environment, 836: 11.

Liu Y.R., Lan X.J., Hou H.Q., Ji J.H., Liu X.M., Lv Z.Z. (2024): Multifaceted ability of organic fertilizers to improve crop productivity and abiotic stress tolerance: review and perspectives. Agronomy-Basel, 14: 28.

Liu Z.C., Shan X.C., Zhao D.T., Zan F.X., Guo G., Wang Z.P., Zhang W., Miao L. (2024): Evaluate the partial nitrification/anammox biofilm system treating the anaerobic biogas slurry of multisource organic solid waste. Journal of Water Process Engineering, 57: 8.

Liu Z.Y., Xu P.D., Yang C.Y., Zhao B.Q., Gao J., Shi L., Dong K.H., Zhao X., Liu F.W., Xu M.G. (2026): Soil organic carbon sequestration efficiency with biochar addition across the croplands of China: a perspective from particulate and mineral-associated organic carbon. Environmental Research, 293: 9.

Lu R. (2000): Methods of Soil and Agro-Chemical Analysis. Beijing, China Agricultural Science and Technology Press.

Lugato E., Lavallee J.M., Haddix M.L., Panagos P., Cotrufo M.F. (2021): Different climate sensitivity of particulate and mineral-associated soil organic matter. Nature Geoscience, 14: 295–300.

Lyu H., Zhong R.H., Kilasara M., Hartono A., Sun Z., Funakawa S., Watanabe T. (2024): Impact of climate on soil organic matter composition in soils of tropical volcanic regions revealed by EGA-MS and Py-GC/MS. Environmental Science and Technology, 58: 9646–9657.

Moller H.B., Sorensen P., Olesen J.E., Petersen S.O., Nyor T., Sommer S.G. (2022): Agricultural biogas production-climate and environmental impacts. Sustainability, 14: 24.

Mou Z.J., Hao Y.Y., Chen X.L., Wang T., Turner B.L., Kandeler E., Lambers H., Liu Z.F. (2025): Climate and pedogenesis exert divergent controls on dissolved organic matter during long-term ecosystem development. Catena, 254: 11.

Moyano F.E., Manzoni S., Chenu C. (2013): Responses of soil heterotrophic respiration to moisture availability: an exploration of processes and models. Soil Biology and Biochemistry, 59: 72–85.

Mukhtiar A., Mahmood A., Zia M.A., Ameen M., Dong R.J., Shoujun Y., Javaid M.M., Khan B.A., Nadeem M.A. (2024): Role of biogas

https://doi.org/10.17221/380/2026-PSE

slurry to reclaim soil properties providing an eco-friendly approach for crop productivity. Bioresource Technology Reports, 25: 14.

Otto A., Simpson M.J. (2006): Evaluation of CuO oxidation parameters for determining the source and stage of lignin degradation in soil. Biogeochemistry, 80: 121–142.

Otto A., Simpson M.J. (2006): Sources and composition of hydrolysable aliphatic lipids and phenols in soils from western Canada. Organic Geochemistry, 37: 385–407.

Post-Beittenmiller D. (1996): Biochemistry and molecular biology of wax production in plants. Annual Review of Plant Physiology and Plant Molecular Biology, 47: 405–430.

Ren T.T., Liao J.H., Delgado-Baquerizo M., Ni J.P., Li Y.Y., Jin L., Ruan H.H. (2023): Organic fertilization promotes the accumulation of soil particulate organic carbon in a 9-year plantation experiment. Land Degradation and Development, 34: 4741–4750.

Saritpongteerak K., Boonsawang P., Sung S.W., Chaiprapat S. (2014): Co-fermentation of oil palm lignocellulosic residue with pig manure in anaerobic leach bed reactor for fatty acid production. Energy Conversion and Management, 84: 354–362.

Schmidt M.W.I., Torn M.S., Abiven S., Dittmar T., Guggenberger G., Janssens I.A., Kleber M., Kögel-Knabner I., Lehmann J., Manning D.A.C., Nannipieri P., Rasse D.P., Weiner S., Trumbore S.E. (2011): Persistence of soil organic matter as an ecosystem property. Nature 478: 49–56.

Shang Y.W., Liang Z., Siddique I.A., Dippold M., Abalos D., Olesen J.E. (2026): Microbial and plant-derived carbon contributions to particulate and mineral-associated organic carbon in perennial and annual cropping systems. Geoderma, 466: 10.

Six J., Conant R.T., Paul E.A., Paustian K. (2002): Stabilization mechanisms of soil organic matter: implications for C-saturation of soils. Plant and Soil, 241: 155–176.

Sun Y.Y., Zhang W.M., Xiu L.Q., Gu W.Q., Wu D., Tang L., Chen W.F. (2025): Long-term fertilization regimes modulate dissolved organic matter molecular chemodiversity and greenhouse gas emissions in paddy soil. Biochar, 7: 15.

Tambone F., Adani F., Gigliotti G., Volpe D., Fabbri C., Provenzano M.R. (2013): Organic matter characterization during the anaerobic digestion of different biomasses by means of CPMAS ^{13}C NMR spectroscopy. Biomass and Bioenergy, 48: 111–120.

Wang D., Wang J., Zhang Y.T., Chen X.P., Chen J., Shi X.J. (2025): Nitrogen-induced soil acidification reduces soil carbon persistence by shifting microbial keystone taxa and increasing Calcium leaching. Agronomy-Basel, 15: 19.

Wen Y.J., Liu X., Yang N., Li Y.P., Zhang J.C. (2025): The contribution of microbial- and plant-derived carbon to soil organic carbon fractions and stability under manure application combined with straw incorporation. Agronomy-Basel, 15: 18.

Wiesenberg G.L.B., Dorodnikov M., Kuzyakov Y. (2010): Source determination of lipids in bulk soil and soil density fractions after four years of wheat cropping. Geoderma, 156: 267–277.

Wiesenberg G.L.B., Gocke M., Kuzyakov Y. (2010): Fast incorporation of root-derived lipids and fatty acids into soil – evidence from a short term multiple $^{14}CO_2$ pulse labelling experiment. Organic Geochemistry, 41: 1049–1055.

Wiesenberg G.L.B., Schneckenberger K., Schwark L., Kuzyakov Y. (2012): Use of molecular ratios to identify changes in fatty acid composition of *Miscanthus* × *giganteus* (Greef et Deu.) plant tissue, rhizosphere and root-free soil during a laboratory experiment. Organic Geochemistry, 46: 1–11.

Wu J., Wang H., Li G., Wu J., Gong Y., Wei X., Lu Y. (2021): Responses of CH_4 flux and microbial diversity to changes in rainfall amount and frequencies in a wet meadow in the Tibetan Plateau. Catena, 202: 105253.

Xie W.H., Ji G.M., Chen F.Q. (2013): The soil labile organic carbon fractions at the different ages of Tea in Three Gorges Reservoir area. 3rd International Conference on Energy. Environment and Sustainable Development (EESD 2013), Shanghai, Trans Tech Publications Ltd.

Xu P., Wu J., Wang H., Tang S., Cheng W., Li M., Bu R., Han S., Geng M. (2023): Combined application of chemical fertilizer with green manure increased the stabilization of organic carbon in the organo-mineral complexes of paddy soil. Environmental Science and Pollution Research, 30: 2676–2684.

Xu W.Z., Zhu Y.Q., Wang X., Ji L., Wang H., Yao L., Lin C.W. (2021): The effect of biogas slurry application on biomass production and forage quality of *Lolium multiflorum*. Sustainability, 13: 13.

Yang Y., Dou Y.X., Wang B.R., Wang Y.Q., Liang C., An S.S., Soromotin A., Kuzyakov Y. (2022): Increasing contribution of microbial residues to soil organic carbon in grassland restoration chronosequence. Soil Biology and Biochemistry, 170: 14.

Yu M.X., Wang Y.P., Deng Q., Jiang J., Cao N.N., Tang X.L., Zhang D.Q., Yan J.H. (2024): Soil acidification enhanced soil carbon sequestration through increased mineral protection. Plant and Soil, 503: 529–544..

Zeng Y.L., Hu Y.T., Wu H.L., Hu B.A., Ouyang S. (2026): Unraveling the divergent contributions of plant- and microbial-derived carbon to soil organic carbon during subtropical vegetation restoration. Land Degradation and Development,37: 2981-2995.

Zhao G.X., Tariq A., Zhang Z.H., Nazim M., Graciano C., Sardans J., Dong X.P., Gao Y.J., Peñuelas J., Zeng F.J. (2025): Afforestation with xerophytic shrubs promoted soil organic carbon stability in a hyper-arid environment of desert. Land Degradation and Development, 36: 655–667.

Zhou Z.H., Ren C.J., Wang C.K., Delgado-Baquerizo M., Luo Y.Q., Luo Z.K., Du Z.G., Zhu B., Yang Y.H., Jiao S., Zhao F.Z., Cai A.D., Yang G.H., Wei G.H. (2024): Global turnover of soil mineral-associated and particulate organic carbon. Nature Communications, 15: 9.

Zhu X.H., Guo Z.Y., Wang N.N., Liu J.Z., Zuo Y.J., Li K.X., Song C.C., Song Y.Y., Gong C., Xu X.F., Yuan F.H., Zhang L.H. (2023): Environmental stress stimulates microbial activities as indicated by cyclopropane fatty acid enhancement. Science of the Total Environment, 873: 11.

Received: August 11, 2026
Accepted: October 22, 2026
Published online: November 20, 2026